CHARACTERISTIC INTERACTION STRUCTURES IN GIBBS TEXTURE MODELLING*

GEORGY GIMEL'FARB†

Abstract. Under the assumption that spatially homogeneous image textures are modelled by Gibbs random fields with multiple pairwise pixel interactions, parallel and sequential schemes of learning a characteristic interaction structure are compared. The learning can be based on a comparison of relative interaction energies or other integral characteristics of each interaction, for instance, chi-square distances between certain grey level difference or cooccurrence histograms collected over a given training sample. Parallel thresholding selects a basic structure of stronger, that is, more energetic or distant, interactions that is sufficient to model a specific class of stochastic textures introduced in [3, 4]. In many cases the basic structure is larger than is required because it contains not only the strong primary interactions but also the sufficiently strong secondary interactions obtained by a statistical interplay of the primary ones. Empirical sequential learning proposed by Zalesny [6, 7] tends to exclude the secondary interactions so that the basic structure can be reduced in size and complemented with a fine structure that describes minor but visually important repetitive details of a texture. The empirical sequential scheme that involves a great body of computations can be approximated by less complex analytical and combined analytical–empirical sequential schemes. Experiments show that the sequential learning results in more precise Gibbs models of non-stochastic regular textures but does not improve (and sometimes may even deteriorate) the basic structure of stochastic textures.

Key words. Texture, Gibbs random field, pairwise interaction, interaction structure.

1. Introduction. We restrict our consideration to a probabilistic image model that describes spatially homogeneous textures as samples of particular Gibbs random fields with multiple pairwise pixel interactions [3, 4]. The model parameters specifying the geometric structure and quantitative strengths of interactions can be estimated, or learned, from a given training sample of the texture. In this paper we discuss the estimation of most characteristic interaction structures.

The structure is usually represented with a neighbourhood graph in which vertices are pixels and edges connect the interacting pixel pairs, called neighbours [2]. The neighbours of a particular pixel directly effect conditional probabilities of grey levels in the pixel. Each pair of neighbours is the second-order clique of the neighbourhood graph, and a spatially homogeneous interaction structure consists of several clique families, each family containing the translation invariant cliques.

Each clique family has its own Gibbs potential that specifies quantitative strengths of pixel interactions in a clique. Generally, the potential values depend on grey level co-occurrences (GLC) in the two pixels. In the simplified case, they depend only on grey level differences (GLD). The sum of the potential values over a clique family, called the partial interaction energy, determines the contribution of the clique family to the Gibbs probability of a particular image.

As shown in [3, 4], the maximum likelihood estimate of the potential for a clique family is closely approximated by the scaled difference between two histograms, namely, between (*i*) the GLCH or GLDH, respectively, collected over a given training sample of the texture and (*ii*) the like expected histogram for the independent random field (IRF). The higher the difference, the greater the impact of the interaction on

*This work was supported in part by the University of Auckland Research Committee grant 9343/3414113.

†Centre for Image Technology and Robotics (CITR), Department of Computer Science, Tamaki Campus, University of Auckland, Private Bag 92019, Auckland 1, New Zealand (g.gimelfarb@auckland.ac.nz)

the Gibbs probability of the training sample. Therefore the characteristic interaction structure can be learned by comparing the partial Gibbs energies (or other integral measures of the difference between the histograms, such as the chi-square distance) for a large search set of possible clique families.

The class of stochastic textures defined in [3, 4] is efficiently described by its basic interaction structure that consists of the clique families with the partial Gibbs energies over a particular threshold. Practically the same structures are recovered by thresholding the chi-square distances between the GLCHs or GLDHs for the training sample and the expected histograms for the IRF. The threshold is chosen using the relative frequency distribution of the Gibbs energies or chi-square distances for all the clique families in the search set [3, 4].

Regular textures such as mosaics mostly do not belong to the class of stochastic textures because they have also a fine interaction structure. The fine structure describes minor but visually important repetitive details, and usually the corresponding clique families have much lower interaction energies than the basic ones. Empirical sequential learning proposed by Zalesny [6, 7] tries to both reduce the basic structure and find the fine structure at the expense of a great body of computations.

In what follows the purely empirical sequential learning is compared to an approximate analytical scheme that involves much less computations and to a combined analytical–empirical sequential scheme. Experiments are conducted with digitized fragments of the stochastic texture D29 "Beach sand" and the regular textures D1 "Woven aluminum wire" and D101 "Cane" [1].

2. Basic notation. Let $\mathbf{R} = [i = (x, y) : \ x = 0, \ldots, M-1; \ y = 0, \ldots, N-1]$ be a finite arithmetic $M \times N$ lattice supporting images. Every clique family $\mathbf{C}_a = \{(i, j) : \ (i, j) \in \mathbf{R}^2; \ i - j = \mathrm{const}_a\}$ consists of the translation invariant cliques (i, j) with the fixed relative shift between the pixels $(i, j) \in \mathbf{C}_a$ denoted

$$\mathrm{const}_a \equiv (\Delta x_a, \Delta y_a).$$

Spatially homogeneous structure $\mathbf{C} = [\mathbf{C}_a \ : \ a \in \mathbf{A}]$ of pairwise interactions is specified by a particular subset $\mathbf{A}$ of the clique families chosen from a large search set $\mathbf{W}$. The search set includes all the families with the bounded inter-pixel shifts $\{(\Delta x, \Delta y) : \ |\Delta x| \le \Delta x_{\max}; \ |\Delta y| \le \Delta y_{\max}\}$. In our experiments the search set $\mathbf{W}$ contains 3280 clique families within the bounds $\Delta x_{\max} = 40, \Delta y_{\max} = 40$.

Let $\mathbf{Q} = \{0, 1, \ldots, q_{max}\}$ and $\mathbf{D} = \{-q_{\max}, \ldots, -1, 0, 1, \ldots, q_{max}\}$ be finite sets of grey levels and GLDs, respectively. Let $\mathbf{g} = [g_i : \ i \in \mathbf{R}; \ g_i \in \mathbf{Q}]$ denote a digital greyscale image. The partial interaction energy $E_a(\mathbf{g})$ of the clique family $\mathbf{C}_a$ in the image $\mathbf{g}$ is as follows:

$$(2.1) \quad E_a(\mathbf{g}) = \mathbf{V}_a \bullet \mathbf{H}_a(\mathbf{g}) = \begin{cases} \sum\limits_{(i,j)\in\mathbf{C}_a} V_a(g_i - g_j) = \sum\limits_{d\in\mathbf{D}} V_a(d) H_a(d|\mathbf{g}); \\ \sum\limits_{(i,j)\in\mathbf{C}_a} V_a(g_i, g_j) = \sum\limits_{(q,s)\in\mathbf{Q}^2} V_a(q, s) H_a(q, s|\mathbf{g}) \end{cases}$$

where $\bullet$ denotes the dot product, $\mathbf{V}_a$ is a Gibbs potential for the clique family $\mathbf{C}_a$ with values depending on the GLCs $(q = g_i, s = g_j)$ or GLDs $d = g_i - g_j$:

$$\mathbf{V}_a = [\, V_a(d) \ : \ d \in \mathbf{D} \,] \quad \text{or} \quad [\, V_a(q, s) \ : \ (q, s) \in \mathbf{Q}^2 \,],$$

and $\mathbf{H}_a(\mathbf{g})$ is the GLDH or GLCH for the family $\mathbf{C}_a$ collected over the image $\mathbf{g}$:

$$\mathbf{H}_a(\mathbf{g}) = [\, H_a(d|\mathbf{g}) \ : \ d \in \mathbf{D} \,] \quad \text{or} \quad [\, H_a(q, s|\mathbf{g}) \ : \ (q, s) \in \mathbf{Q}^2 \,].$$

Let $\mathbf{V} = [\mathbf{V}_a : a \in \mathbf{A}]$ and $\mathbf{H}(\mathbf{g}) = [\mathbf{H}_a(\mathbf{g}) : a \in \mathbf{A}]$ denote the potential vector and the GLDH or GLCH vector, respectively. The GLDH- or GLCH-based Gibbs image model with multiple pairwise pixel interactions [3, 4], specified by an interaction structure $\mathbf{C}$ and potential $\mathbf{V}$, relates the Gibbs probability of every sample $\mathbf{g}$:

$$\Pr(\mathbf{g}|\mathbf{C},\mathbf{V}) = \frac{1}{Z_{\mathbf{C},\mathbf{V}}} \exp\left(E(\mathbf{g})\right) \tag{2.2}$$

to the total interaction energy $E(\mathbf{g})$ of the sample:

$$E(\mathbf{g}) = \sum_{a \in \mathbf{A}} E_a(\mathbf{g}) = \mathbf{V} \bullet \mathbf{H}(\mathbf{g}). \tag{2.3}$$

As shown in [3, 4], the analytical first approximation of the MLE of the potential $\mathbf{V}_a$ for the GLDH-based or GLCH-based Gibbs model of Eq. (2.2), given a training sample $\mathbf{g}^\circ$, is proportional to the difference $\mathbf{H}_a(\mathbf{g}^\circ) - \mathbf{H}_{a,\mathrm{irf}}$ where $\mathbf{H}_{a,\mathrm{irf}}$ denotes the expected triangular GLDH or the uniform GLCH, respectively, for the IRF. The IRF is described by the model of Eq. (2.2) with zero-valued potentials $\mathbf{V} = \mathbf{0}$.

For brevity, the image simulation by the GLCH-based or GLDH-based model in Eqs. (2.2) and (2.3) is called below the GLC-simulation and GLD-simulation, respectively. The simulation is performed by the Controllable Simulated Annealing (CSA) introduced in [4] and based on the stochastic gradient algorithm proposed by Younes [5]. The CSA generates a nonstationary Markov chain of images by the conventional stochastic relaxation, namely, by the Metropolis sampler [2], but adapts concurrently the potential $\mathbf{V}$. The potential is changed at each macrostep in such a way as to achieve a stochastic approximation of the GLDHs or GLCHs $\{\mathbf{H}_a(\mathbf{g}^\circ) : a \in \mathbf{A}\}$ for the training sample with the like histograms for the simulated images. Each macrostep traces randomly, but without repetitions, all the pixels $i \in \mathbf{R}$. The approximation takes account of only the clique families that comprise the characteristic interaction structure of the Gibbs model. In the experiments below, each simulation uses 300 macrosteps of the CSA with the same control parameters as were used for experiments in [4]. Below all the training and simulated samples are of size 128×128 pixels, unless otherwise specified.

3. Learning the interaction structures. The basic characteristic interaction structure of a stochastic texture is recovered by comparing the partial Gibbs energies to the threshold $\theta = E_{\mathrm{m}} + k\sigma$ depending on their frequency distribution over the search set $\mathbf{W}$. Here, E_{m} and σ are the mean energy and standard deviation, respectively. In our experiments the factor k is mostly chosen within the range $3 \le k \le 5$.

The approximate analytical estimate of the relative partial energy $e_a(\mathbf{g}^\circ)$ for a clique family $\mathbf{C}_a$ in a given training sample $\mathbf{g}^\circ$ is as follows [4]:

$$e_a(\mathbf{g}^\circ) = \mathbf{H}_a(\mathbf{g}^\circ) \bullet (\mathbf{H}_a(\mathbf{g}^\circ) - \mathbf{H}_{a,\mathrm{irf}}). \tag{3.1}$$

Practically the same basic structures are recovered by thresholding the chi-square distances $\chi^2_a(\mathbf{H}_a(\mathbf{g}^\circ), \mathbf{H}_{a,\mathrm{irf}})$ between the GLCHs or GLDHs for the training sample and the IRF.

Figures 3.1 – 3.3 show the training and simulated samples of the textures D29, D1, and D101 [1]. Basic structures of different size, learned for the stochastic texture D29, result in a good visual quality of the simulations that is quite similar for both the GLCH- and GLDH-based models. Here, the top eight clique families in the partial Gibbs energy or the chi-square distance, found with the factor $k = 5$, are

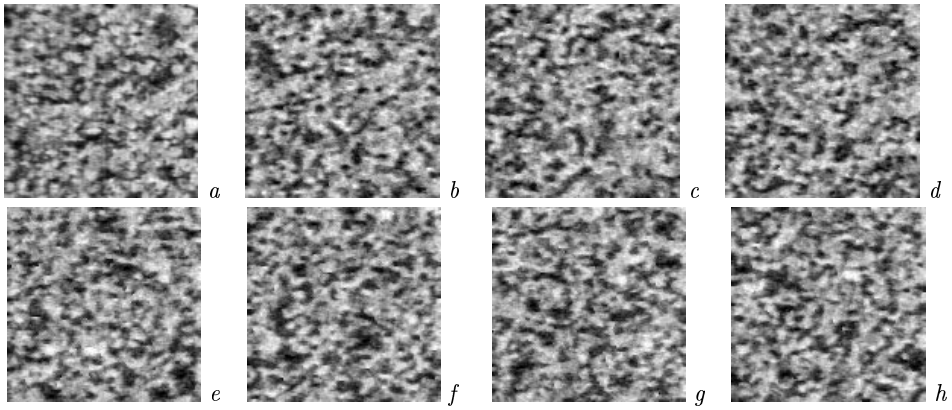

FIG. 3.1. *Texture D29: training sample (a), GLD-simulation with the basic structure of 8 (b), 17 (c), and 24 (d) clique families (thresholding of the chi-square distances to the IRF), and GLC-simulation with the structures of 8 (e,g) and 11 (f,h) families (thresholding of the chi-square distances and the partial Gibbs energies, respectively).*

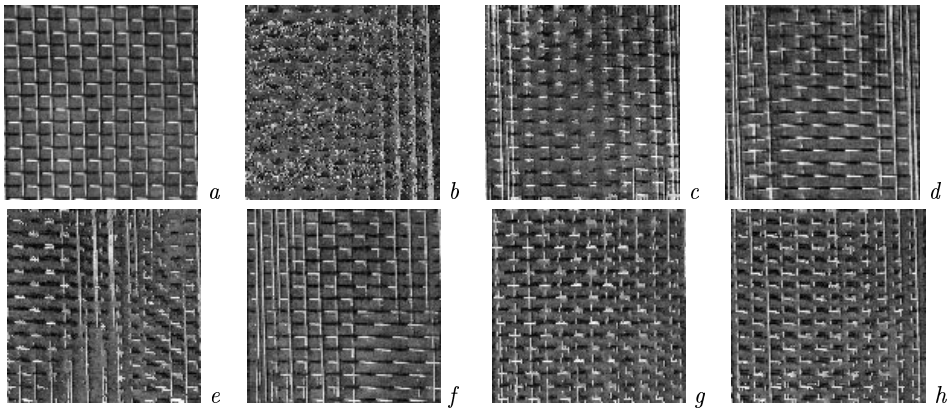

FIG. 3.2. *Texture D1: training sample (a), GLD-simulation with the basic structures of 27 (b) and 40 (c) clique families (thresholding of the chi-square distances) and of 60 (d) families (thresholding of the Gibbs energies), and GLC-simulation with the basic structures of 11 (e), 37 (f), 48 (g), and 73 (h) clique families (thresholding of the chi-square distances).*

just the same, namely, $\{(1,0),(0,1),(-1,1),(1,1),(2,0),(-2,1),(2,1),(0,2)\}$, and the additional families have almost no effect on the descriptive ability of the model.

At the same time the basic structures of the non-stochastic textures D1 and D101 reproduce only very roughly the repetitive original patterns, and the larger sizes of the structure do not significantly improve the simulation. The GLCH-based models of such textures outperform the simplified GLDH-based models because, as shown in [4], the multimodal GLCHs, and thus the potentials for the former models, cannot be closely approximated by the GLDH-based counterparts.

3.1. Sequential learning. This approach is based on the implicit assumption that the interactions can be subdivided into the primary and secondary ones. The primary interactions do describe a particular texture and must appear in the structure. The secondary interactions are created only by statistical interplay of the primary ones and have to be excluded because they do not effect the descriptive abilities of a

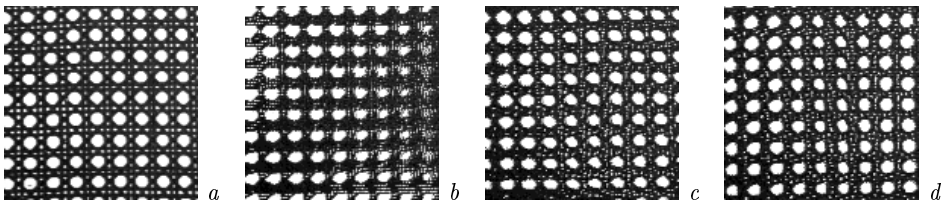

FIG. 3.3. *Texture D101: training sample (a) and GLC-simulation with the basic structures of 19 (b), 39 (c), and 63 (d) clique families (thresholding of the partial Gibbs energies).*

model. Generally, the probability distributions of the GLCs or GLDs for the various clique families cannot be statistically independent. But if the dependence between the primary families can be ignored, the basic structure can be reduced in size and the fine structure can be recovered by successively eliminating the secondary interactions produced by a current set of the primary ones.

Let the primary clique families $\mathbf{C}_\alpha$ and $\mathbf{C}_\beta$ have significant partial energies in a given training sample. Then the secondary family $\mathbf{C}_\gamma$, such that $\text{const}_\gamma = \text{const}_\alpha + \text{const}_\beta$, will usually possess a significant but somewhat lower energy, too, although this family may not appear in the structure. In other words, if the GLDHs or GLCHs $\mathbf{H}_\alpha(\mathbf{g}^\circ)$ and $\mathbf{H}_\beta(\mathbf{g}^\circ)$ differ much from the expected histograms for the IRF, the similar difference for the histogram $\mathbf{H}_\gamma(\mathbf{g}^\circ)$ is also expected to be large.

The parallel thresholding does not discriminate between the primary and secondary interactions. Thus it cannot detect the necessary components of the basic and fine interaction structures that rank below the secondary interactions in the partial Gibbs energy of Eq. (2.1) or the chi-square distance to the IRF.

The empirical sequential learning, proposed by Zalesny [6, 7], tries to iteratively detect and eliminate the secondary interactions for reducing the basic structure to only the primary interactions and recovering thus the fine interaction structure.

3.1.1. Empirical scheme. At every iteration of the empirical sequential learning, a single clique family that is the most characteristic with respect to a previously found interaction structure, is added to the structure. An iteration t consists of the two successive steps.

1. (*Texture simulation*) A new texture sample $\mathbf{g}^{[t]}$ is GLD- or GLC-simulated under a current interaction structure $\mathbf{C}^{[t]} = \{\mathbf{C}_a : a \in \mathbf{A}^{[t]}\}$.
2. (*Structure selection*) The GLDHs or GLCHs $\{\mathbf{H}_a(\mathbf{g}^\circ) : a \in \mathbf{A}^{[t]}\}$ for a given training sample $\mathbf{g}^\circ$ are compared to the like histograms $\{\mathbf{H}_a(\mathbf{g}^{[t]}) : a \in \mathbf{A}^{[t]}\}$ for the simulated sample $\mathbf{g}^{[t]}$ to select the most characteristic clique family and add it to the current structure.

The comparison can be based, in particular, on the maximum relative partial energy

$$e_a(\mathbf{g}^\circ) = \mathbf{H}_a(\mathbf{g}^\circ) \bullet (\mathbf{H}_a(\mathbf{g}^\circ) - \mathbf{H}_a(\mathbf{g}^{[t]})) \tag{3.2}$$

or the chi-square distance $\chi^2_a(\mathbf{H}_a(\mathbf{g}^\circ), \mathbf{H}_a(\mathbf{g}^{[t]})$ between the histograms.

In principle, the simulation step takes account of all the dependences between the interactions so that the structure of the minimum size is expected to be found. But this empirical scheme involves a large body of computations for simulating the samples as the number of samples to be generated is equal to the size of the final structure. Also, the GLD- or GLC-simulation under a fixed interaction structure $\mathbf{C}^{[t]}$ produces a variety of different samples $\mathbf{g}^{[t]}$. The GLDHs or GLCHs $\mathbf{H}_a(\mathbf{g}^{[t]})$ for these samples

are distributed around and approach only in average the like histograms for a given training sample. Therefore the selected clique families will reflect also a particular sequence of simulated images, and the same training sample may give rise to different interaction structures, especially, as concerning the fine structure.

3.1.2. Approximate analytical scheme. Generally, the GLD or GLC distributions over the different clique families are statistically dependent even for the IRF. But some of the actual dependences are rather weak, and we may assume that the primary clique families have the independent GLC distributions. Then the GLC distributions for the secondary interactions can be approximately obtained from the primary ones by recomputing each current secondary GLCH, $\mathbf{H}_\gamma(\mathbf{g})$, using the last chosen primary GLCH, $\mathbf{H}_\alpha(\mathbf{g})$, and the corresponding previous primary or secondary GLCH, $\mathbf{H}_\beta(\mathbf{g})$, such that $\text{const}_\gamma = \text{const}_\alpha + \text{const}_\beta$. In this case all the GLCHs in the search set $\mathbf{W}$ can be analytically updated after adding to a current interaction structure the next clique family with the maximum relative energy of Eq. (3.2) or with the maximum chi-square distance with respect to the training sample.

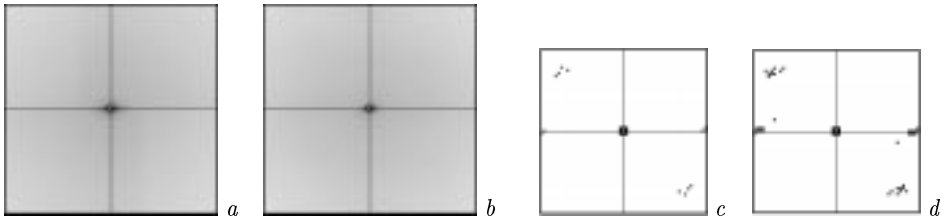

FIG. 3.4. *Texture D29: the computed (a) and actual (b) Gibbs energies for the GLCH-based Gibbs model with the 10 analytically chosen clique families and the analytically chosen structures of the 10 (c) and 22 (d) clique families with the top relative energy.*

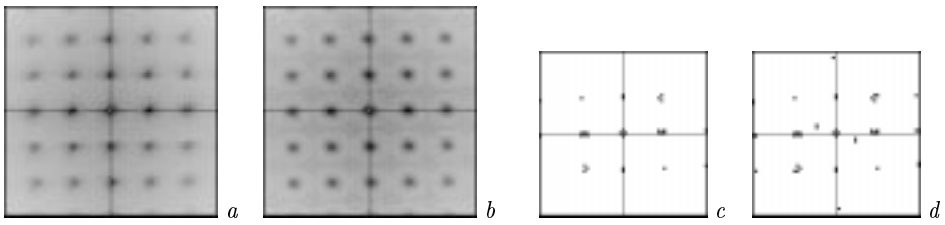

FIG. 3.5. *Texture D101: computed (a) and actual (b) Gibbs energies for the GLCH-based Gibbs model with the 15 analytically chosen clique families and the analytically chosen structures of the 15 (c) and 22 (d) clique families with the top relative energy.*

Figures 3.4, *a*-*b*, and 3.5, *a*-*b*, demonstrate the grey-coded actual and analytically computed distributions of the relative partial energies of Eq. (3.1) for the textures D29 and D101 over the search set $\mathbf{W}$. This latter set is displayed as the 325×325 window, each square box 4×4 representing a particular inter-pixel shift $(\Delta x, \Delta y)$; $-40 \leq \Delta x, \Delta y \leq 40$. The computations of the secondary GLCHs are propagated from the centre to the borders of the window $\mathbf{W}$ to roughly approximate the main part of the statistical interplay between the primary interactions.

The energy distributions for the textures D29 and D101 are computed, respectively, with the 10 and 15 primary clique families. These families were sequentially selected by choosing at each step the family with the maximum relative energy of

Eq. (3.1). The corresponding interaction structures as well as the more detailed structures with the 22 clique families are shown in Figures 3.4, *c-d*, and 3.5, *c-d*.

In these examples the reduced basic structure of the texture D29 contains the two highly energetic clique families $\{(1,0),(0,1)\}$. All other families are two or more orders of magnitude lower in the relative energies so that the chosen fine structure of this texture contains only the non-characteristic long-range interactions such as $\{(-13,35),(-1,25),(-15,15),(26,11)\}$ and so forth. These latter does not represent specific visual features and are obviously arbitrary, as distinct from the fine structure of the regular texture D101. But, as we shall see later, the analytical sequential learning based on the relative chi-square distances results in more workable interaction structure for the stochastic texture D29.

The analytical sequential scheme gives a reasonable fit to the actual partial Gibbs energies and, therefore, to the GLCHs for the clique families. Therefore it is of interest to compare this scheme to the empirical sequential learning.

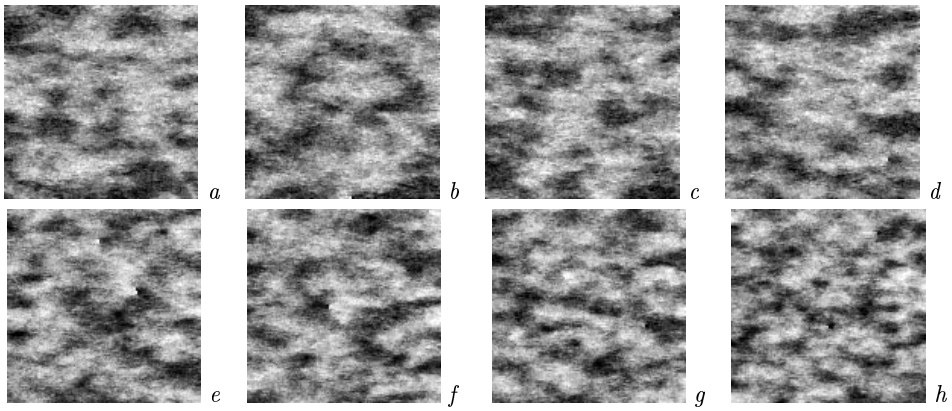

FIG. 4.1. *Texture D29: GLD-simulation with the 2 (a), 3 (b), 5 (c), and 6 (d) clique families and GLC-simulation with the 4 (a), 5 (b), 7 (c), and 11 (d) clique families found by the sequential empirical choice of the top relative Gibbs energy. Notice that these images do not mimic the initial visual pattern of Figure 3.1,* a.

4. Stochastic texture D29: experimental results. Figure 4.1 shows the samples obtained by the GLD- or GLC-simulation after learning the interaction structure from the training sample in Figure 3.1, *a*, by the empirical sequential choice of the clique family with the top relative energy of Eq. (3.1). In this case the actual energy distribution in the search window **W** is closely approximated by the statistical interplay of only the two clique families $\{(1,0),(0,1)\}$. As a result, the additional fine structure is chosen rather arbitrary among the remaining families with very low relative Gibbs energies, and the final structure is unsuitable for simulating the texture samples that are visually similar to the training sample D29 in Figure 3.1, *a*. The images in Figure 4.1, in contrast to the simulated samples in Figure 3.1, differ much from the training sample even when the overall interaction structure is of the same or greater size than the basic structure recovered by thresholding the energies.

At the same time, the empirical sequential choice based on the relative chi-square distances produces more workable interaction structures for the texture D29. The GLD-simulations with the sequentially chosen 1–12 clique families: $[(0,1),\ (1,0),\ (5,0),\ (1,3),\ (8,2),\ (-3,2),\ (-9,1),\ (3,0),\ (-16,9),\ (2,0),\ (3,25),\ (-21,15)]$ are shown in Figure 4.2. The samples simulated with the 8–12 clique families (Figure 4.2, *h-l*)

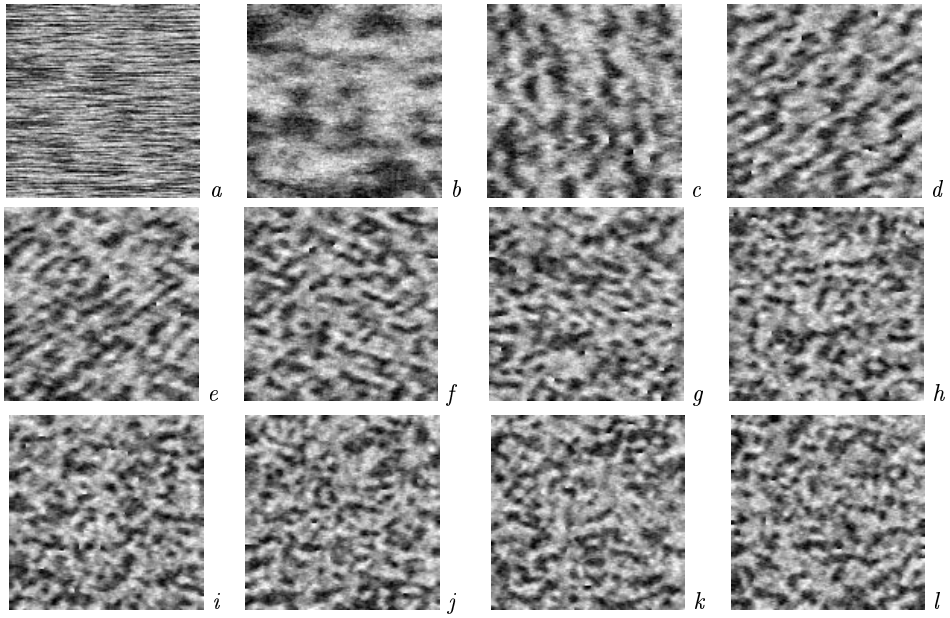

FIG. 4.2. *Texture D29: GLD-simulation with the 1 (a) – 12 (l) clique families found by the sequential empirical choice of the top relative chi-distance. The structures of the 8–12 families produce the samples that are already reasonably similar to the training one.*

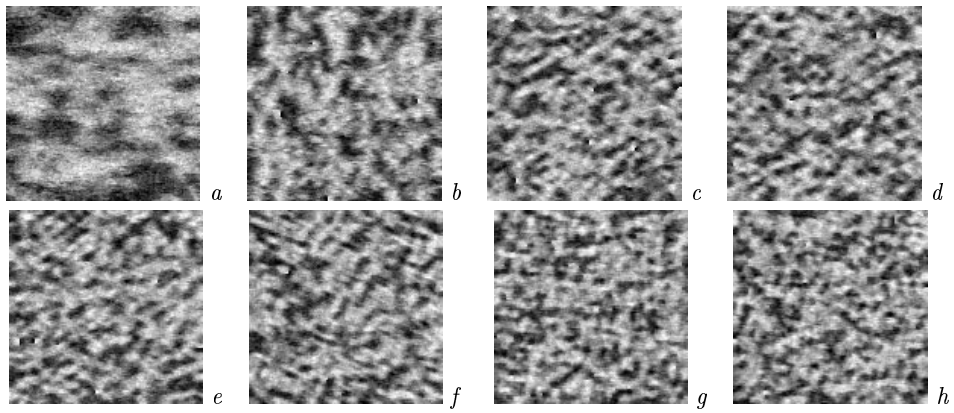

FIG. 4.3. *Texture D29: GLD-simulation with the 2 (a) – 16 (h) clique families found by the sequential empirical choice of the top two relative chi-distances.*

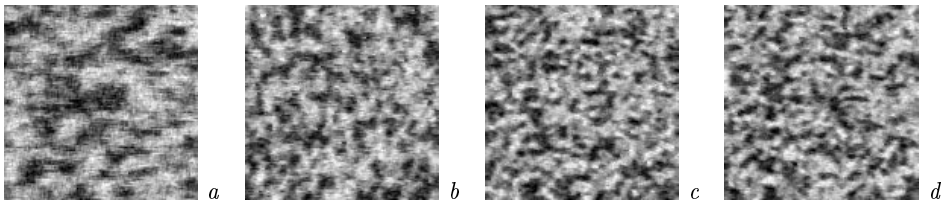

FIG. 4.4. *Texture D29: GLD-simulation with the 4 (a) – 16 (d) clique families found by the sequential empirical choice of the top four relative chi-distances.*

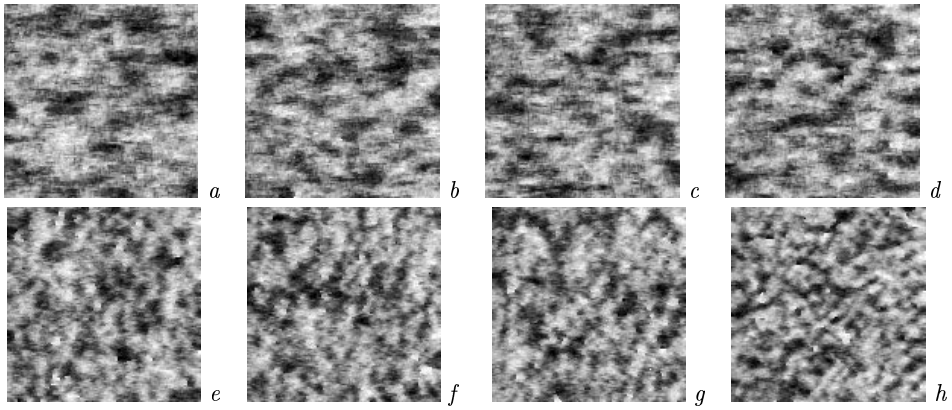

FIG. 4.5. *Texture D29: GLC-simulation with the 4 (a), 10 (b), 15 (c), and 22 (d) clique families found by the analytical sequential choice of the top relative Gibbs energy and with the 6 (e), 9 (f), 12 (g), and 16 (h) families found by the like choice of the top relative chi-square distance.*

are similar to (but subjectively seem still to be a bit worse than) those in Figure 3.1, *b,e,g*, that are GLD- or GLC-simulated with the 8 families $[1,0)$, $(0,1)$, $(-1,1)$, $(1,1)$, $(2,0)$, $(-2,1)$, $(2,1)$, $(0,2)]$ obtained by thresholding the relative Gibbs energies or the relative chi-square distances.

The empirical scheme can be accelerated by choosing the two or the four top-rank clique families in the the relative chi-square distances at each iteration, as shown in Figures 4.3 and 4.4. But the final structures have to be of larger size ($12-16$ families) to approach the same visual quality of simulation as in Figure 4.2, *h-l*.

The analytical sequential search behaves in this case just as the empirical one but produces slightly worse results. Figures 3.1, 3.4, and 4.5 show that the basic structure recovered by the parallel thresholding of the partial energies produces much better simulation results even when the analytically chosen structure is of larger size. The analytical search based on the chi-square distances produces the more appropriate interaction structures but they are still less efficient than the structures recovered by the thresholding. The GLC-simulation with the 16 analytically chosen clique families in Figure 4.5 is similar to the GLD-simulation with the 8-12 empirically found ones in Figure 4.2 as well as with 12-16 families in Figures 4.3 and 4.4.

The possible reason of the ineffective energy-based sequential search is that the assumed statistical dependences of the GLC distributions for the secondary interactions do not properly manifest themselves in the Gibbs energies so that the detection of the primary interactions and exclusion of the secondary ones using the relative energies of Eq. (3.2) is not justified. In this case the sequential learning only deteriorates the actual interaction structure. The relative chi-square distances seem to be more accurate in detecting the secondary interactions. But for this stochastic texture the basic structure found by the parallel thresholding of the partial energies or the chi-square distances to the IRF is still better than (or, at least, gives the same simulation quality as) the empirical or analytical sequential learning.

5. Regular texture D101: experimental results. Figures $5.1-5.3$ present samples produced by the GLD- and GLC-simulation, once the interaction structure of 1–40 or 3–22 clique families, respectively, has been learned by the energy-based empirical sequential search. The training sample D101 is shown in Figure 3.3, *a*. The

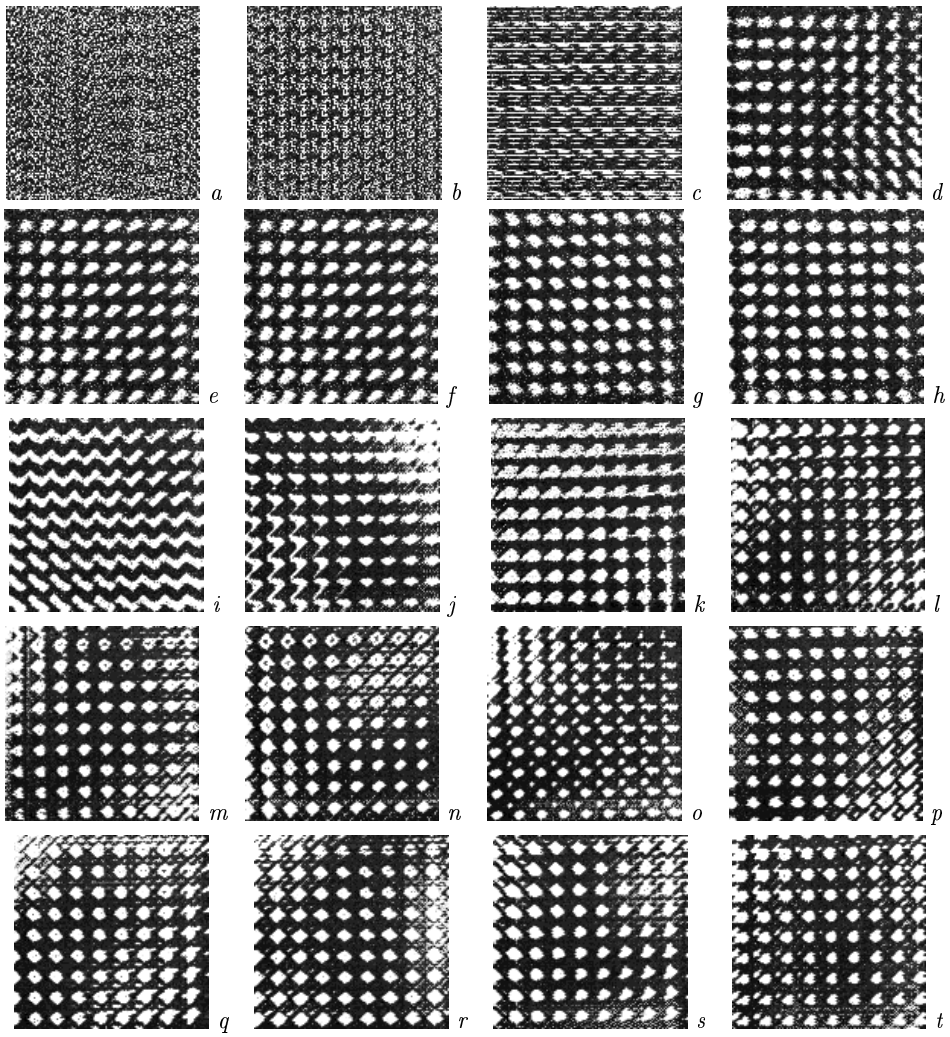

FIG. 5.1. *Texture D101: GLD-simulation with the 1 (a) – 20 (t) clique families found by the sequential empirical choice of the top relative Gibbs energy.*

simulated samples are obtained by adding each time one more clique family with the top relative energy of Eq. (3.1) to the previously found primary interaction structure. Here, the final structures of 19–22 families found by the empirical sequential learning for the GLCH-based model in Figure 5.3, *q*-*t*, both contain less clique families and represent better the fine repetitive details than the basic structure of the 63 families in Figure 3.3, *d*, found by the parallel thresholding of the partial Gibbs energies.

The simplified GLDH-based model ranks far below the GLCH-based one because the GLDHs for a given training sample and therefore the potentials of the GLD-based Gibbs model of Eq. (2.2) cannot be proper representatives of the actually multimodal training GLCHs and the GLC-based potentials [4].

First, the GLDH-based Gibbs model is almost invariant to the greyscale inversion that converts the positive into the negative. As a result, the simulated samples in Figures 5.1 and 5.2 demonstrate continuous spatial transitions from the positive-like

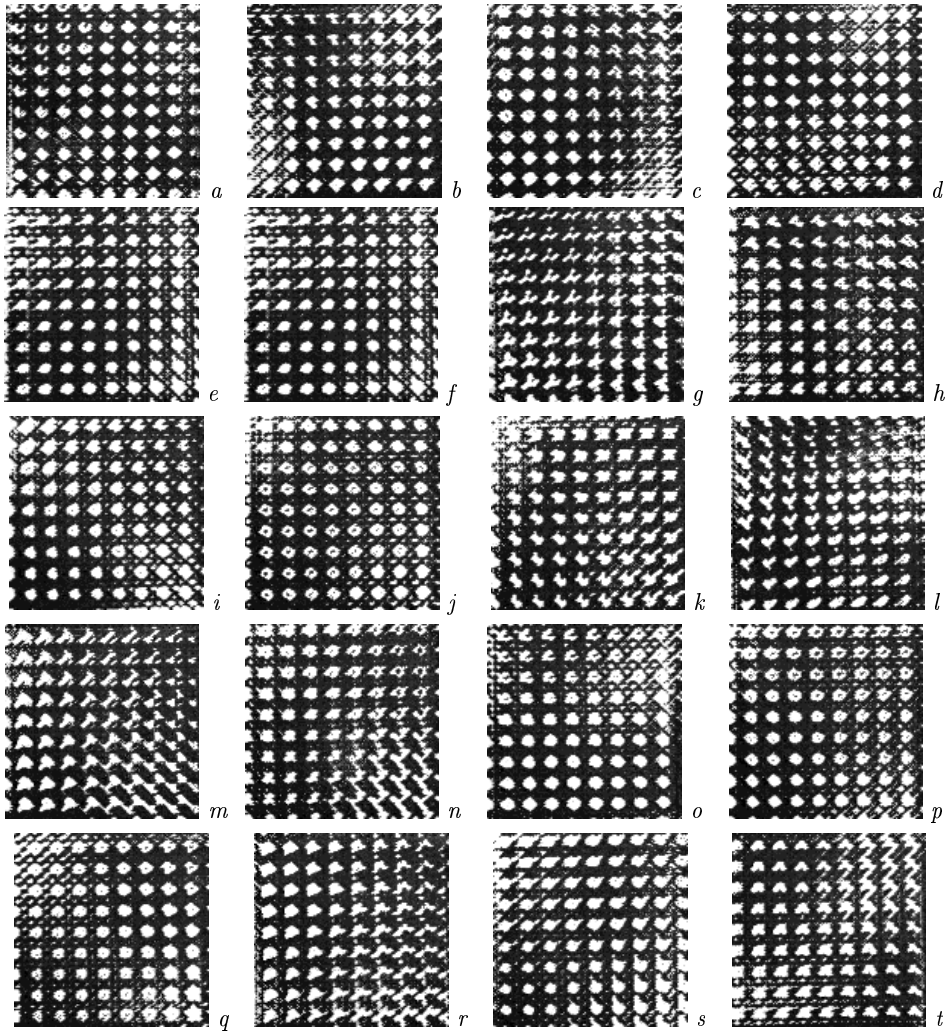

FIG. 5.2. *Texture D101: GLD-simulation with the 21 (a) – 40 (t) clique families found by the sequential empirical choice of the top relative Gibbs energy.*

reproductions of the training pattern to the negative-like ones, and such transitions are obviously absent in the training sample.

Secondly, the interaction structures that are sequentially chosen for the GLDH-based model produce much worse simulation results than the structures of lesser size for the GLCH-based model. Some GLD-simulated samples tend to reflect basic and fine repetitive details of the texture as, for instance, in Figure 5.2, *e, f, i*, obtained with the 25, 29, and 30 clique families, respectively, but the apparently better GLC-simulated samples in Figure 5.3, *q, r*, are obtained using the characteristic structure of only 18–19 clique families.

Thus, from here on, we will discuss only the GLCH-based model of Eq. (2.2). It should be pointed out that the stochastic texture D29 has at most the symmetric unimodal GLCHs and potentials so that both the models give almost the same quality of simulation.

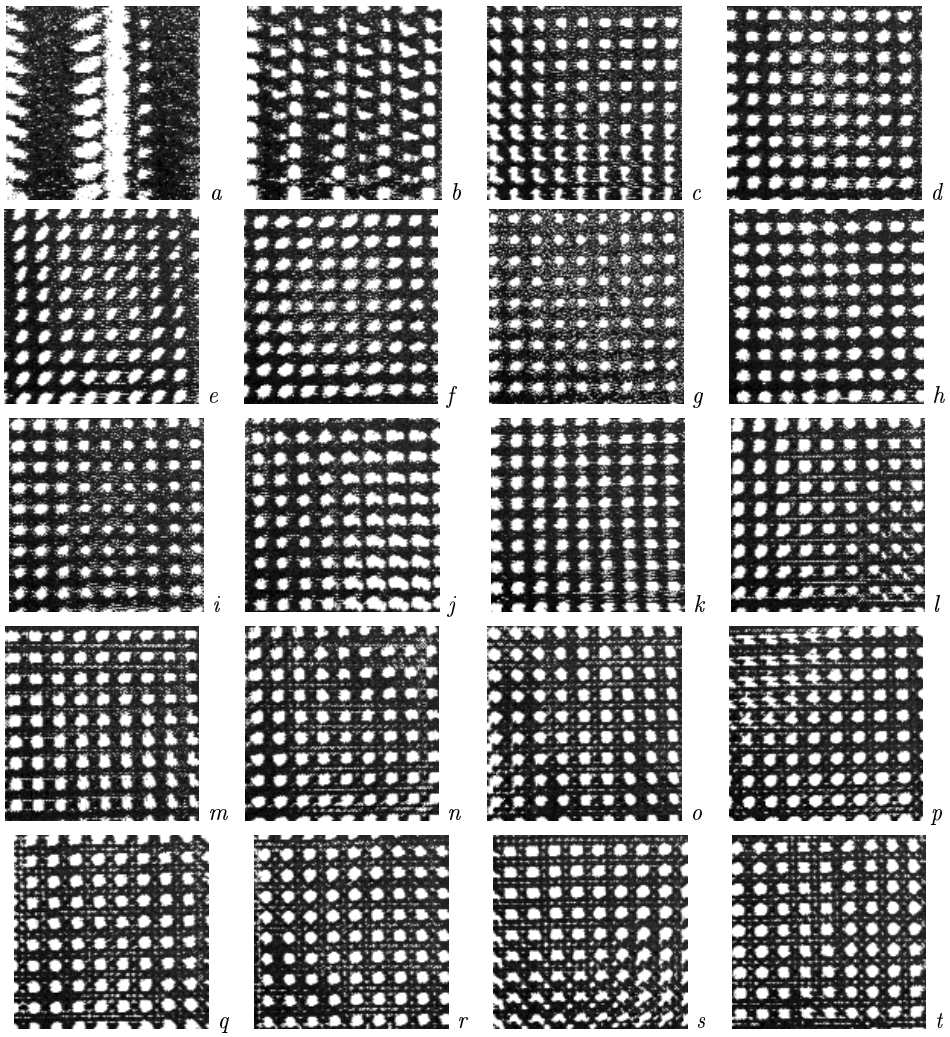

FIG. 5.3. *Texture D101: GLC-simulation with the 3 (a) – 22 (t) clique families found by the sequential empirical choice of the top relative Gibbs energy.*

By comparing Figure 3.3, *c-d*, to Figures 5.3, *a-p*, and 5.3, *q-t*, one can come to the conclusion that the sequential choice of a single clique family with the top relative energy of Eq. (3.2) forms the reduced basic structure of about the 16 clique families and the fine structure of the 4–6 additional clique families. Quite similar results can be obtained twice faster by choosing the two top families at each step (Figure 5.4). But the structures of similar size obtained by choosing more than two clique families per iteration result in a somewhat worse simulation shown in Figure 5.5.

It must be emphasized that the visual quality of simulation does not steadily increase with the structure's size. As follows from Figures 5.3, *n-t*, 5.4, *d–h*, and 5.5, *f–h*, the quality may even significantly degrade after adding a clique family. Usually in our experiments the quality is then restored and improved, once one or two more families are added. But unfortunately, it is still unclear how to relate the visual quality of texture simulation to certain quantitative features of a current interaction

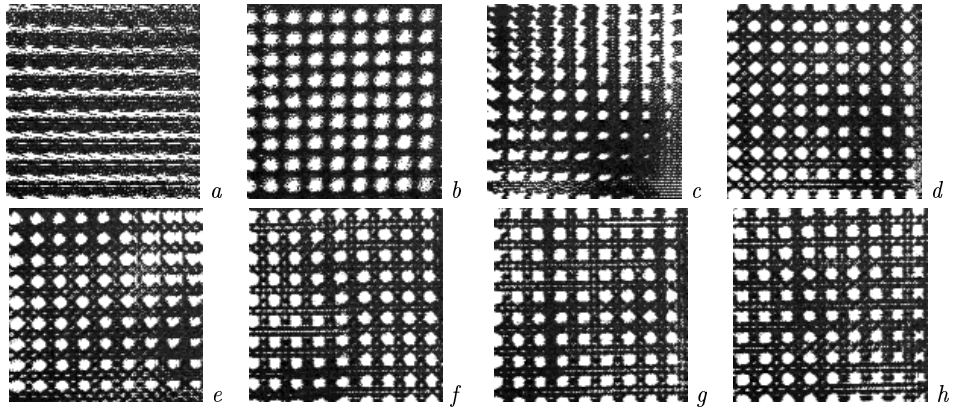

FIG. 5.4. *Texture D101: GLC-simulation with the 4 (a) – 12 (e), 16 (f), 18 (g), and 22 (h) clique families found by the sequential empirical choice of the top two relative Gibbs energies.*

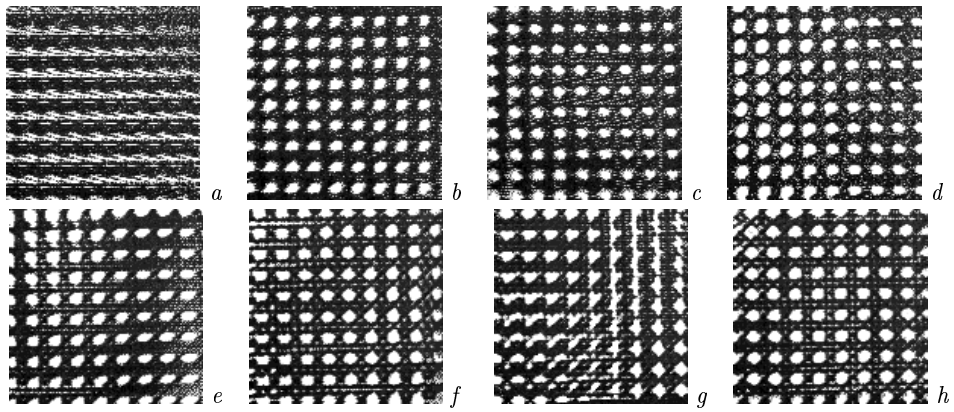

FIG. 5.5. *Texture D101: GLC-simulation with the 4 (a) – 32 (h) clique families found by the sequential empirical choice of the top four relative Gibbs energies.*

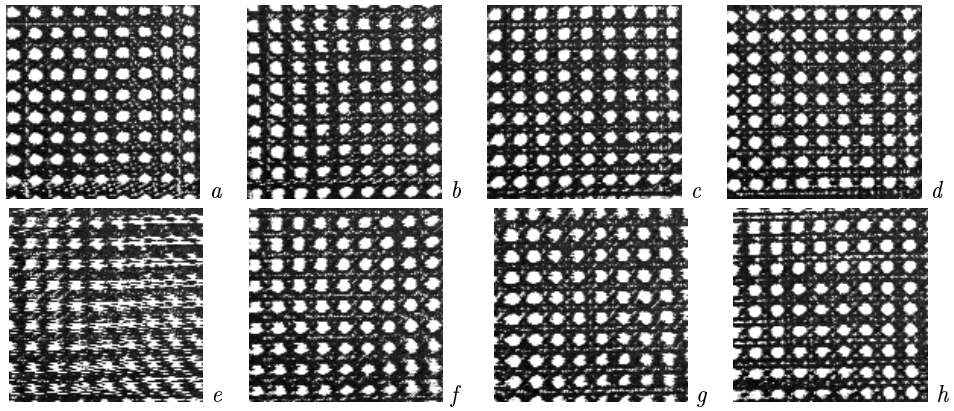

FIG. 5.6. *Texture D101: GLC-simulation with the 15 (a,e), 19 (b,f), 25 (c,g), and 32 (d,h) found by the analytical sequential choice of the top relative Gibbs energy and the top relative chi-square distance, respectively.*

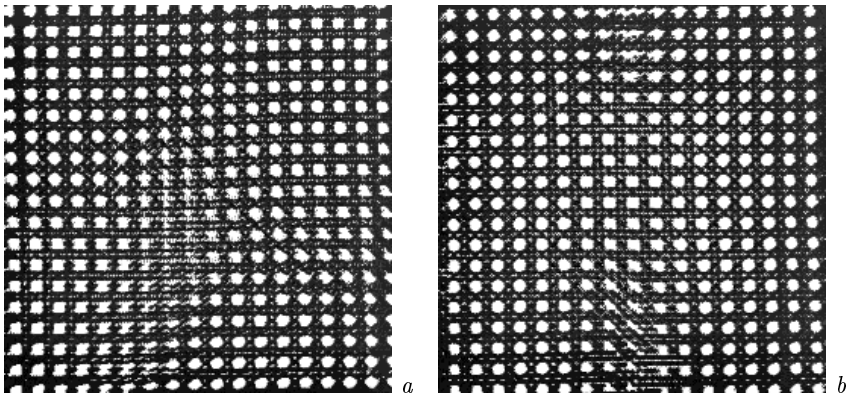

FIG. 5.7. *Texture D101: GLC-simulation with the 40 clique families found by the analytical sequential choice (a) and with the 22 families found by the sequential empirical choice of the top relative Gibbs energy (b).*

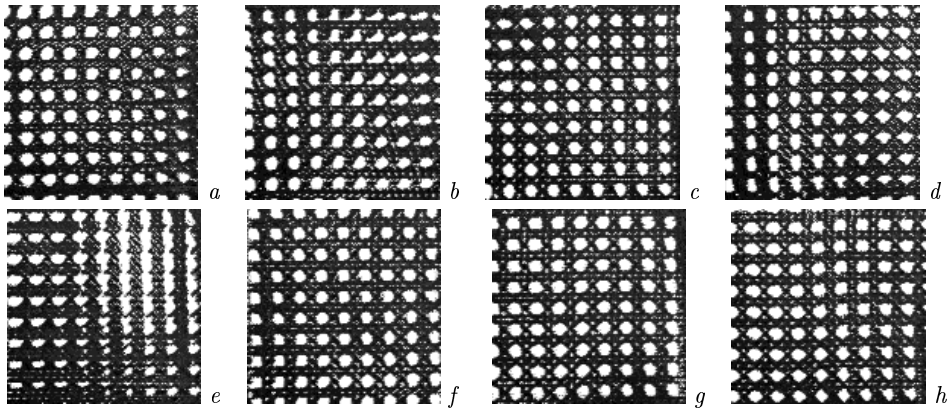

FIG. 5.8. *Texture D101: GLC-simulation with the 15 clique families found by the analytical sequential choice and with the additional 1 (a) – 8 (h) families found by the sequential empirical choice of the relative Gibbs energy.*

structure, for instance, to relative Gibbs energies or chi-square distances for all the clique families in a search set $\mathbf{W}$ at each iteration t of the sequential learning.

The analytical sequential learning in Figure 5.6 creates the basic interaction structures of the 15–19 clique families. The GLC-simulation with these structures produces the samples that are very similar to the samples in Figure 3.3, *c*-*d*, obtained with the 39–63 families. But the additional fine structure is slightly less efficient so that the overall structure of the 32–40 analytically selected clique families is required to produce the results similar to the empirically found structure of the 20–22 families.

For comparison, the samples 256×256 in Figure 5.7 are simulated with the 40 and 22 clique families chosen by the energy-based analytical and empirical search, respectively. The texture in Figure 5.7, *a*, as well as the one in Figure 5.6, *d*, simulated with the 32 clique families do reflect the fine repetitive visual details but to the lesser extent than the samples in Figures 5.3, *o*-*t*, 5.4, *d*-*h*, 5.5, *h*, and 5.7, *b*, obtained by the empirical sequential learning. It is worth noting that the analytical search based on the relative Gibbs energies works here better than the one based on the relative

chi-square distances.

As follows from the above experiments, the sequential learning can produce the efficient interaction structures only if our assumption about the independent primary GLC distributions has a reasonable fit to the textures under consideration. We call these latter the regular textures.

The empirical sequential learning slightly outperforms the faster analytical scheme as concerning the fine interaction structure of a regular texture. But the reduced basic structures recovered empirically or analytically are very similar so that it is worth consideration whether the empirical sequential learning can be accelerated by combining the both approaches.

Figure 5.8 shows the results of simulating the texture D101 when the reduced basic interaction structure with the 15 clique families is found analytically (see, also, Figures 3.5 and 5.6) and then is appended with the fine structure of 1–8 clique families by the empirical sequential learning. In this case the purely empirical and the combined analytical–empirical sequential learning produce very similar final results, but the latter approach is almost three times faster than the former one.

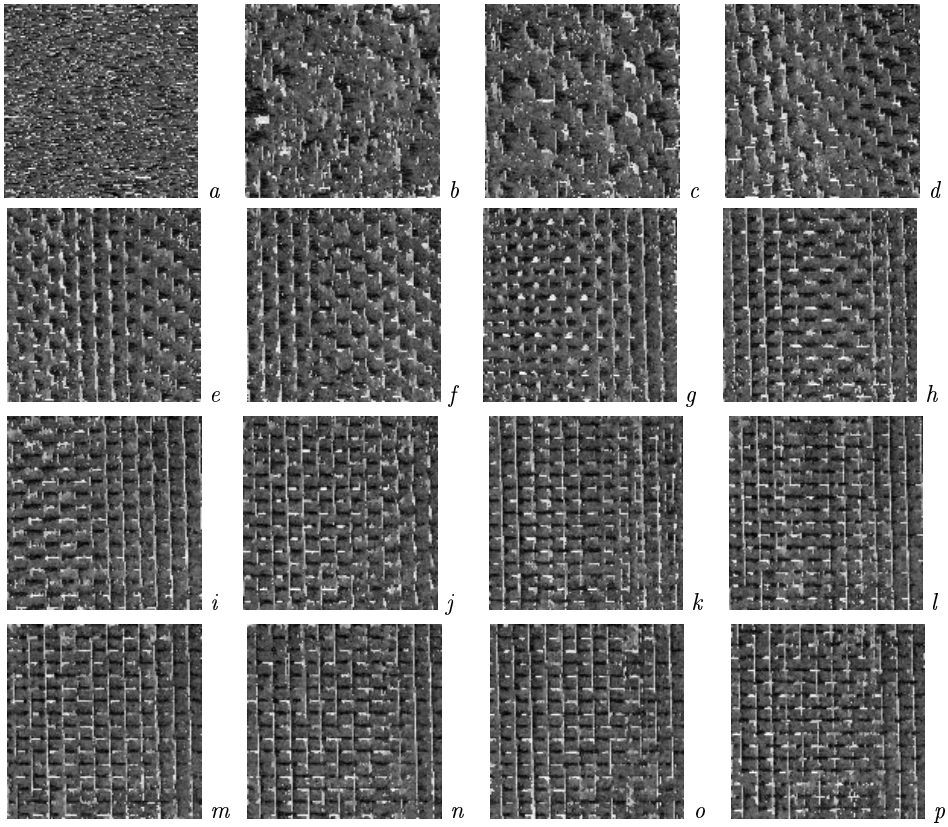

FIG. 6.1. *Texture D1: GLC-simulation with the 1 (a) – 16 (t) clique families found by the sequential empirical choice of the top relative chi-square distance.*

6. Regular texture D1: experimental results. Figures 6.1 and 6.2 show results of the GLC-simulation when the interaction structures of 1–40 clique families are obtained by the empirical sequential search of the top chi-square distance between

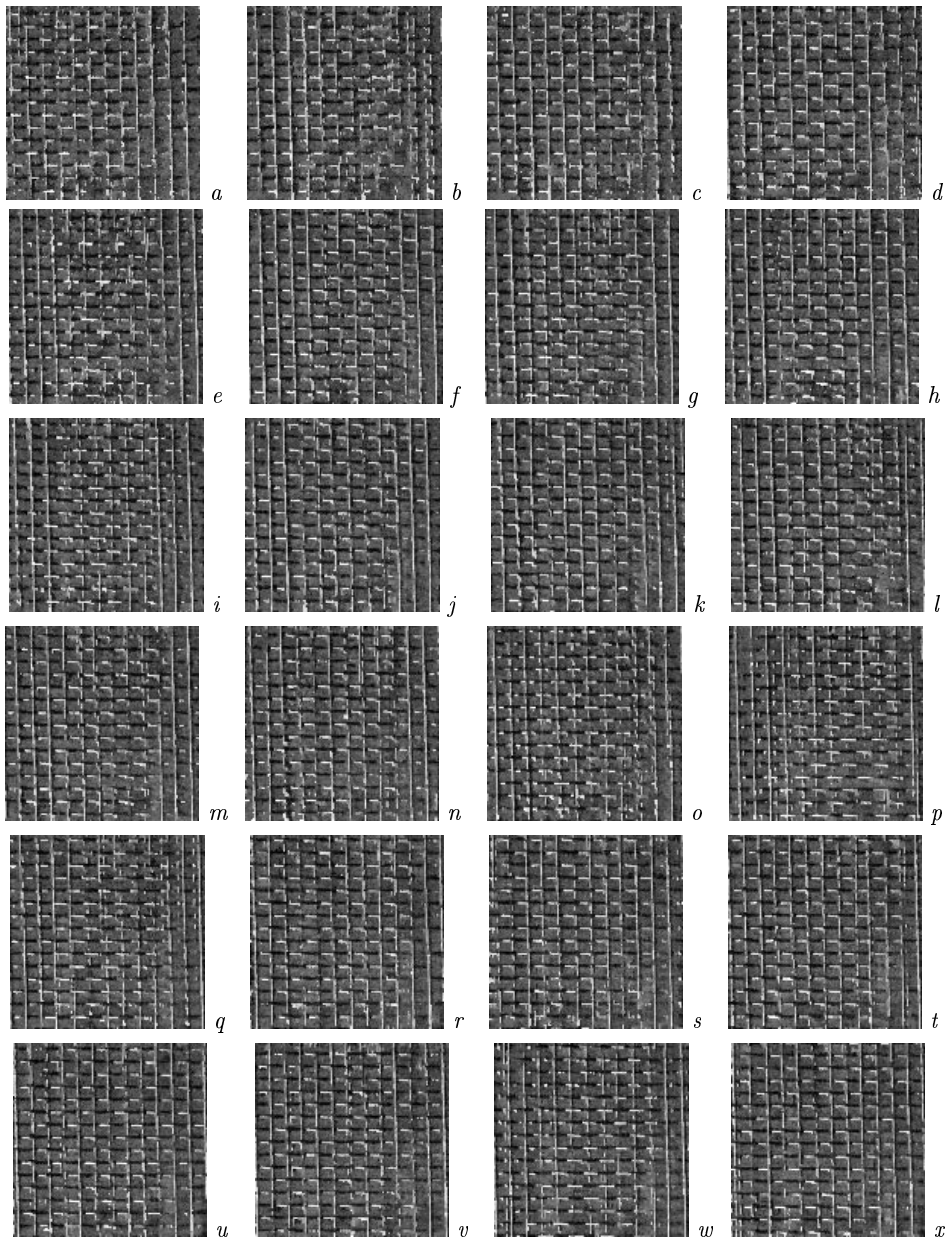

FIG. 6.2. *Texture D1: GLC-simulation with the 17 (a) – 40 (t) clique families found by the sequential empirical choice of the top relative chi-square distance.*

the training and generated GLCHs. The training sample D1 is shown in Figure 3.2. Here, as follows from Figure 3.2, *d, h*, and Figure 6.1, *a*-*p*, the basic structure contains only about 12–16 clique families. But then even the 24–28 additional families give only a rough approximation of the minor details of this texture. There is only a very subtle improvement in visual quality between the samples that are simulated with the additional four clique families in Figure 6.1, *p*, and with the additional 5–24 families in Figure 6.2, *a*–*x*, that form the fine interaction structure of the model.

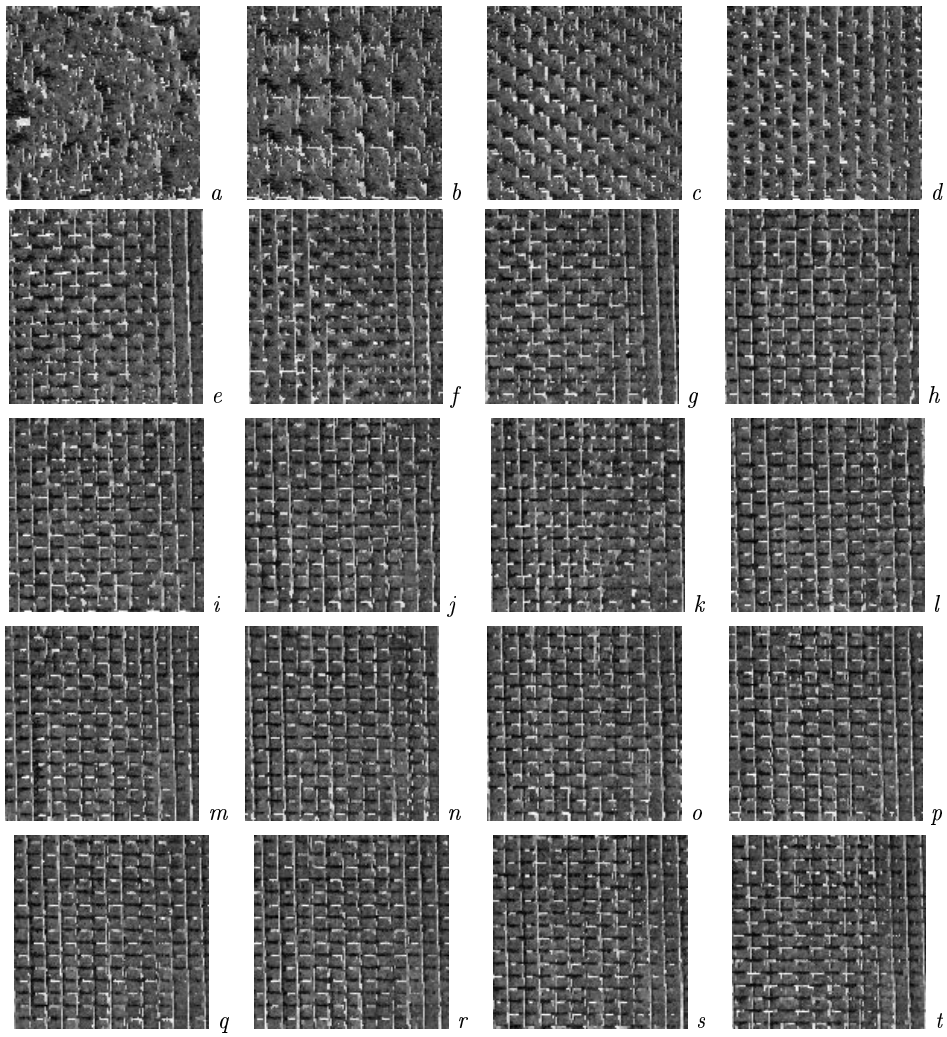

FIG. 6.3. *Texture D1: GLC-simulation with the 2 (a) – 40 (t) clique families found by the sequential empirical choice of the top two relative chi-square distances.*

Although the repetitive details of the texture D1 are reproduced less efficiently than those of the texture D101, the sequential learning by choosing the top-rank clique family in the relative chi-square distance outperforms noticeably the parallel thresholding. The analytical sequential search illustrated by Figure 6.5 presents here a reasonable alternative to the empirical one although the simulated samples have a bit lesser visual quality than the samples in Figure 6.2, *q–t*.

It should be pointed out that in this case both the empirical and analytical sequential choice of the top-rank clique family results in much better interaction structures than the accelerated empirical search for the two or four top-rank families at each iteration, as shown in Figures 6.3 and 6.4, respectively. The combined analytical–empirical schemes shown in Figures 6.6 and 6.6 rank below the purely analytical one, too, as regarding the visual quality of simulation.

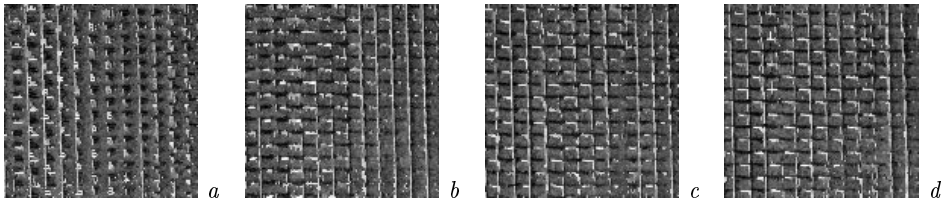

FIG. 6.4. *Texture D1: GLC-simulation with the 8 (a), 16 (b), 24 (c), and 32 (d) clique families found by the empirical sequential choice of the four top relative chi-square distances.*

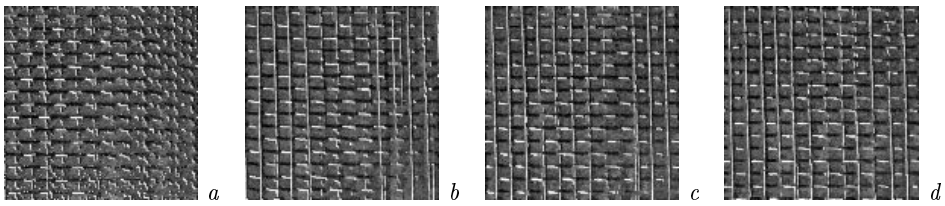

FIG. 6.5. *Texture D1: GLC-simulation with the 14 (a), 26 (b), 34 (c), and 40 (d) clique families found by the analytical sequential choice of the top relative chi-square distances.*

7. Conclusions. These and other experiments, as well as the results in the empirical sequential learning discussed in [7], suggest that spatially homogeneous image textures that are simulated more or less efficiently by the Gibbs model of Eq. (2.2) can be subdivided into the two classes, namely, the stochastic textures and the regular textures. The classes vary in assumed statistical relationships between the different clique families.

To model a stochastic texture, all the clique families with the GLDHs or GLCHs for the training sample that possess sufficiently high partial Gibbs energies or chi-square distances with respect to the IRF have to be treated as statistically independent and included into the basic interaction structure.

The like structure of a regular texture will contain both the independent primary interactions and the dependent secondary interactions produced by a statistical interplay of the primary ones. Thus the basic structure can be reduced in size and the fine interaction structure can be additionally recovered by a sequential elimination of the secondary interactions. The sequential learning can be based on either the relative partial Gibbs energies or chi-square distances between the GLDHs or GLCHs for the training and simulated samples. But in some cases the relative chi-square distances result in slightly better interaction structures.

The separation into the primary and secondary interactions does not improve the modelling of stochastic textures. Moreover, the energy-based sequential learning may even deteriorate the interaction structure of such textures comparing to the parallel thresholding or even to the sequential schemes based on the chi-square distances.

The empirical sequential learning requires a substantial amount of computations. Also, each characteristic structure produced by the empirical scheme reflects a particular chain of the sequentially generated samples. Therefore the same training sample may result in rather different characteristic structures. The alternative analytical sequential learning is much faster but reproduces only approximately the actual relations between the primary and secondary interactions. Therefore, to approach, if possible at all, the simulation quality of the empirical learning, the analytical scheme

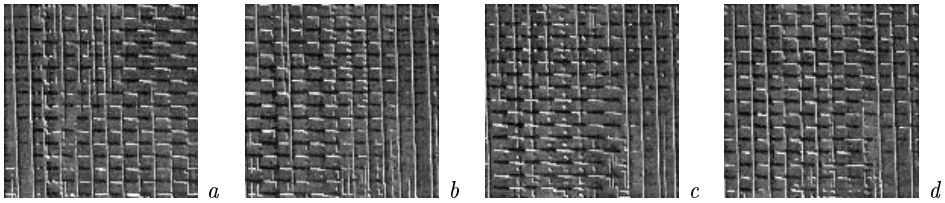

FIG. 6.6. *Texture D1: GLC-simulation with the 14 families found by the analytical sequential choice of the top relative chi-square distances and with the addtitional 8 (e), 9 (f), 10 (g), and 11 (h) families found by the like empirical choice.*

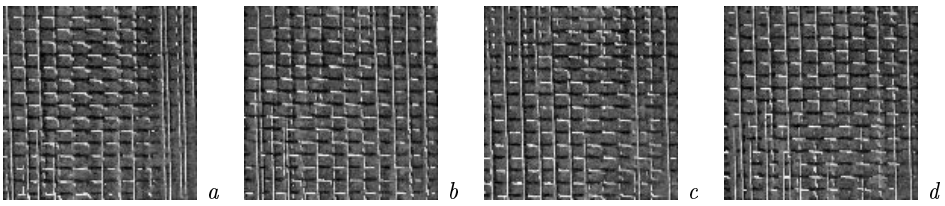

FIG. 6.7. *Texture D1: GLC-simulation with the 26 clique families found by the analytical sequential choice of the top relative chi-square distances and with the additional 2 (i), 4 (j), 7 (k), and 8 (l) families found by the empirical choice by the sequential thresholding of the relative distances with* $k = 4$.

has to produce the characteristic structures of larger size. The combined analytical–empirical schemes mostly do not behave better than the purely analytical one.

It should be noted that all the sequential schemes as well as the parallel thresholding have no theoretically justified rules of how to choose a proper size of the interaction structure. Thus the number of the clique families to be included into the Gibbs model of a particular texture is selected, mainly, on the experimental base.

Our experiments and the experiments in [4, 7] show that the classes of stochastic and regular textures include many natural images. But a rich variety of textures that are outside these classes should be modelled by other means.

REFERENCES

[1] P. Brodatz, *Textures: A Photographic Album for Artists and Designers.* Dover Publications, New York, 1966.

[2] R. Chellappa, A. Jain (Eds), *Markov Random Fields: Theory and Application.* Academic Press, Boston, 1993.

[3] G. L. Gimel'farb, "Texture modeling by multiple pairwise pixel interactions", *IEEE Transactions on Pattern Analysis and Machine Intelligence*, 18:1110–1114, 1996.

[4] G. L. Gimel'farb. *Image Textures and Gibbs Random Fields.* Kluwer Academic Publishers, Dordrecht, 1999.

[5] L. Younes. "Estimation and annealing for Gibbsian fields", *Annales de l'Institut Henri Poincaré – Probabilités et Statistiques*, 24: 269–294, 1988.

[6] A. V. Zalesny. *Personal communication.* 1998.

[7] A. V. Zalesny. Analysis and synthesis of textures with pairwise signal interactions. Project 50542 (EC ACTS 074 "Vanguard"). Technical Report. Katholieke Univ. Leuven, 1999.